

FOG Design Report

Fluorescencia desde Órbita Geoestacionaria

Hernán Asorey, Xavier Bertou, Mariano Gomez Berisso

*CNEA / CONICET / UNCuyo / UNRN
Centro Atómico Bariloche, Argentina*

Federico Sanchez, Manuel Platino

*CNEA / CONICET / UNSAM
Centro Atómico Constituyentes, Argentina*

April 13,2010

Contents

Executive Summary	3
1 Scientific Objectives	4
1.1 Fluorescence background measurements	4
1.2 Terrestrial Fluorescent flashes	6
1.2.1 Transient Luminous Events	6
1.2.2 Tatiana UV Flashes	8
1.3 Gamma Ray Bursts	8
2 Detector Description	10
2.1 Optics design	10
2.2 Electronics	10
2.2.1 Analog electronics	10
2.2.2 Digital electronics	12
2.2.3 Power consumption and temperature considerations	12
2.3 Packaging	13
2.4 Detector Simulation	14
3 Detector Operation	16
3.1 Duty Cycle	16
3.2 Online data processing	17
3.2.1 Calibration	17
3.2.2 Fluorescence background	17
3.2.3 Terrestrial flashes	17
3.2.4 Gamma Ray Bursts	18
3.3 Fault tolerance	18
3.4 Telemetry	18
4 Organisation, Costs and Schedule	20
4.1 Project Organisation	20
4.2 Project Schedule	21
4.3 FOG Costs	21
4.4 Publication policy	22
4.5 Manpower	23
Bibliography	24

Executive Summary

One of the most active topics in Astrophysics is the field of ultra high energy cosmic rays (UHECR), where Argentina plays a key role with the Pierre Auger Observatory. First results of the Observatory have opened the road to the charged particles astronomy, but the event rates are low and a definitive identification of the UHECR sources will only be possible with huge observatories of hundreds of square kilometres. To reach such a large instrumented area, the only proven technique is the use of fluorescence telescopes as in Auger and other cosmic ray experiments, but looking at Earth from space, searching for tracks of ultra violet (UV) light as the cosmic rays cascade through the atmosphere.

While the GEO orbit of ARSAT satellites is too distant from Earth to allow such a measurement, it is ideal to observe a significant fraction of the total Earth atmosphere in order to establish the UV background that fluorescence telescopes from space will have to face. The UV flux is such that a small telescope of ~ 15 cm of diameter will focus enough photons to produce a measurable signal in a multi anode photomultiplier tube (MAPMT). By using a 4×4 MAPMT, one can measure different areas on Earth and study effects such as cloud related albedo. This document describes such a detector to be placed in ACTA (Arreglo de Cargas Tecnológicas Argentinas) in the ARSAT-1 satellite. The instrument is called FOG for Fluorescencia desde Órbita Geostacionaria, Fluorescence from a Geostationary Orbit in Spanish.

In addition to this measurement, such a telescope can detect UV flashes from Earth. Many intriguing phenomenas happening above thunderclouds are known to produce UV flashes and the fluxes are such that FOG would be an ideal detector to measure them. Other sources of UV flashes have been proposed in the literature and FOG data will be of high relevance to identify eventual burst from sources such as tectonic movements or gamma ray bursts (GRB).

FOG is a compact $24 \text{ cm} \times 28 \text{ cm} \times 29 \text{ cm}$ apparatus of an estimated total weight below 8.5 kg. It has been designed with low power consumption in mind, staying below 7 W in operation, and below 50 W h integrated over a full day. To reduce the needs in telemetry, strong data processing will be done at the level of the local data acquisition (DAQ) in order to stay below 4 bps. The design has been optimised to minimise the impact on ACTA and ARSAT-1.

1 Scientific Objectives

The main scientific objective of FOG is to characterise the UV emission of the atmosphere as seen from space looking for time and space variations. Most measurements up to now either have a good timing resolution but are done from low orbit with a small field of view, or are long integration measurement from a far distance. Using a fast MAPMT one would be able to observe both spacial variations and evolution with time.

On top of the observation and characterisation of this continuous and supposedly slowly changing background, one can add a specific program of observation of fast variations on millisecond timescales. Local (UV flashes) and potentially global (GRB) flashes have different progenitors and through their observation different physic topics are at test.

1.1 Fluorescence background measurements

The ultra high energy cosmic rays (UHECR) are elementary particles (ex. proton) or nuclei (ex. iron), with energies up to at least 10^{20} eV. When they reach the Earth atmosphere, they produce a cascade of secondary particles, mainly gammas, electrons, positrons and muons. They can be detected either by installing particle detectors at ground, or by looking at the trace they leave in the atmosphere: they excite nitrogen molecules which then de-excite producing fluorescence light. At the highest energies these UHECR are expected to travel almost in straight line in the universe, being only slightly deflected by the galactic and extra galactic magnetic fields. Furthermore, above 6×10^{19} eV, one expects the UHECR to interact with the cosmic microwave background and lose energy over a few tens of Mpc. One would therefore expect only few events above this energy threshold, called the GZK cutoff[1]. The few events above the GZK are then expected to come from the nearby universe, less than 100 Mpc away, in almost straight line.

The Pierre Auger Observatory, with its 3000 km^2 close to Malargüe, in the south of the Mendoza Province, Argentina, is up to this day the largest cosmic ray observatory. It combines the two techniques of detection: an array of 1600 surface detector stations on a triangular grid, spaced by 1500 m, that sample the lateral distribution of UHECR cascades, and 24 fluorescence telescopes that observe at night the longitudinal development of these cascades. The first results of the Pierre Auger Observatory indicate that the UHECR are probably accelerated in astrophysical sites within a few 100 Mpc of the Earth, given the anisotropy of the arrival direction of the highest energy events[2] and the clear observation of a flux suppression at 6×10^{19} eV, as expected from the GZK[3]. Other results such as the non observation of photons and neutrinos as UHECR also point towards this scenario.

In order to go further away and identify the sources of these UHECR, huge detectors are needed. The flux of events at the Pierre Auger Observatory is about 20 events per year, orders of magnitude lower than what is needed to be able to identify sources. The northern site of the Pierre Auger Observatory is foreseen to instrument 20000 km^2 , 7 times the southern site. However, this is still relatively small and it becomes difficult to instrument larger areas on ground. One idea, studied since the 80s[4], is to use the same fluorescence technique used by the Pierre Auger Observatory (and other experiments before such as the Fly's Eye and Hires), but instrument the telescope in space, looking down over the Earth atmosphere. This allows to reach hundreds of thousands of square kilometres. Various projects are about to implement this technique. While it is not clear if TUS[5] or OWL[6] will fly soon, JEM-EUSO[7] is likely to be installed on the international space station in 2015.

In this context, it is of great importance to characterise the fluorescence background these satellites will face. While some generic data is already available from ground based measurements, these are only available in some specific sites. A first measurement from space was done by the Russian satellite Tatiana[8]. The measurement was made by a single PMT, from a LEO orbit. It gave interesting results on how the background light depends on the moon illumination, and measurements of the light contamination by cities. It also detected UV flashes whose origins are still under debate (see 1.2 below).

FOG would complement these data with measurement from a GEO orbit. The GEO orbit has the

advantage of always looking at the same area, allowing to increase the statistics day after day and a better control over systematic biases. The location of ARSAT-1 will allow FOG to see dark area of land (amazonian region), of ocean, and regions more densely populated. By using a MAPMT, FOG can observe these various areas at the same time. The field of view of a 4×4 MAPMT is shown on figure 1. The 4 corner pixels are blinded to measure the background of cosmic rays direct hit to the PMT, while the other 12 pixels observe different areas of the Earth atmosphere, covering about 60 degrees in longitude and latitude.

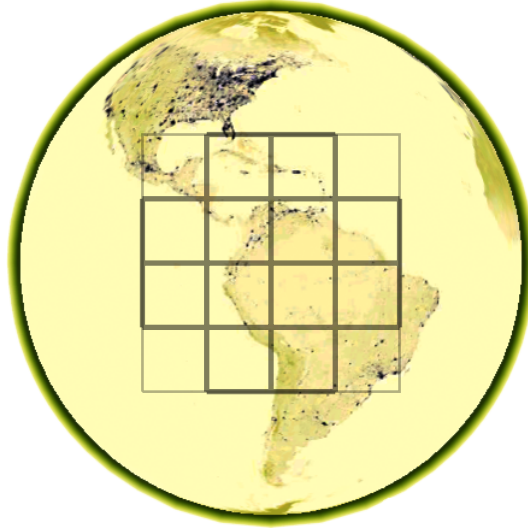


Figure 1: FOG field of view from ARSAT-1 position. The background Earth is a negative image of the city lights as obtained by NASA in visible light. The 4×4 pixels are drawn on the Earth surface. The 4 corner pixels will be blinded.

The relevant data to be retrieved in order to understand better the fluorescence background for JEM-EUSO and other similar projects would be the evolution of the background pixel by pixel as a function of time and moon phase. Hourly histograms will indicate differences between each area on Earth. The evolution of these histograms as a function of time will help understanding the options of taking data during twilight periods to increase the duty cycle. Short time correlations will be studied to look for correlated noise that could produce spurious triggers in a space-borne fluorescence telescope.

From Tatiana data, one can compute the expected flux at the level of the GEO orbit of ARSAT-1. The average background rate derived from Tatiana data is between 3×10^7 and 10^8 photons/cm²/s/sr[8], with some important variations depending on the moon illumination and the albedo of the Earth (for example, depending on cloud coverage). Big cities can increase the background light by a factor of 2, while a full moon can increase it by a factor up to 30. The 950 km orbit of the satellite is 37.7 times closer to Earth than ARSAT-1 GEO orbit, and therefore one can expect a flux at the GEO orbit $37.7^2 = 1420$ times lower. Considering the extreme cases, one gets a flux at the FOG position \mathcal{F}_F :

$$2 \times 10^4 \text{ photons cm}^{-2} \text{ s}^{-1} \text{ sr}^{-1} < \mathcal{F}_F < 2 \times 10^6 \text{ photons cm}^{-2} \text{ s}^{-1} \text{ sr}^{-1}$$

Using the field of view per pixel of figure 1, and a 15 cm diameter mirror concentrator (see 2.1 for a more detailed description of the optical system proposed), one gets a flux of events at the level of a pixel of the MAPMT of 3 to 300 kHz for each pixel.

1.2 Terrestrial Fluorescent flashes

1.2.1 Transient Luminous Events

Since the 60's, brief optical emissions above thunderstorms have been observed [9]. These emissions are manifestations of intense energy exchanges between the atmospheric layers, and in general are called *Transient Luminous Events* (TLEs): flashes of optical emissions in the stratosphere and mesosphere above severe thunderstorms. Figure 2 shows different types of TLEs: sprites, jets, elves, halos, and gigantic blue jets (GBJs). The relevant scale lengths for this TLEs range from a few meters to hundreds of kilometres, with interval duration from fractions of microseconds to almost one second [10].

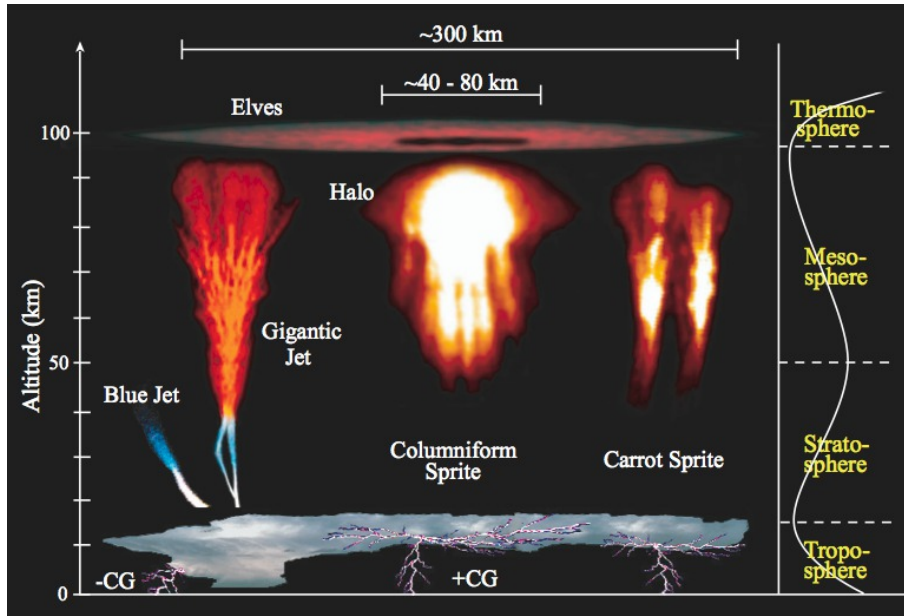


Figure 2: Different types of TLEs: sprites, jets, elves, GBJs (from Ref. [11]).

During the past years, several thousands of TLEs have been observed on different ground-based missions. In particular, more than 400 TLEs were observed above one thunderstorm system over north-eastern Argentina [12]. However, the only way for measuring TLEs at global scale in the high energy electromagnetic spectrum (NUV, FUV, X and gamma emissions) is by space-based observations campaigns on board the ISS (like the Lightning and Sprite Observations Experiment - LSO - in the years 2001 to 2004), the Space Shuttle (for example, the Mediterranean Israeli Dust Experiment - MEIDEX - during the STS-107 mission) or by dedicated space missions (TARANIS and ASIM). A complete review is available in [13].

The geographical distribution of TLEs is shown in figure 3. TLEs mainly occurs over areas where thunderstorms are observed, but exhibit different local distribution for different types of TLEs: halos are mainly observed over the coastlines and oceans; sprites above continents; and elves mainly above oceans when the sea surface exceeds 26°C , indicating an ionosphere-ocean coupling. The ISUAL instrument (Image of Sprites and Upper Atmospheric Lightning), on-board the FORMOSAT-2 satellite, measured the global occurrences rates for the different types of TLEs: 3.23, 0.50, 0.39 and 0.01 events per minute for elves, sprites, halos and GBJs, respectively[14].

TLEs spectrum is characterised by emissions in the visible and near infrared band (NIR), and in the NUV band[15], as shown on Figure 4. Since TLEs are produced at high altitude in the atmosphere ($\gtrsim 30$ km), little atmospheric attenuation is expected when looked from above, making FOG very sensitive to these phenomenas.

Considering that a GBJ radiates $\sim 10^{25}$ NUV photons in a cone of 10 degrees of aperture, from an altitude of ~ 50 km [17], one can estimate the total fluence at GEO orbit to be $F_{\text{GBJ}} \sim 2 \times 10^6$ ph cm^{-2}

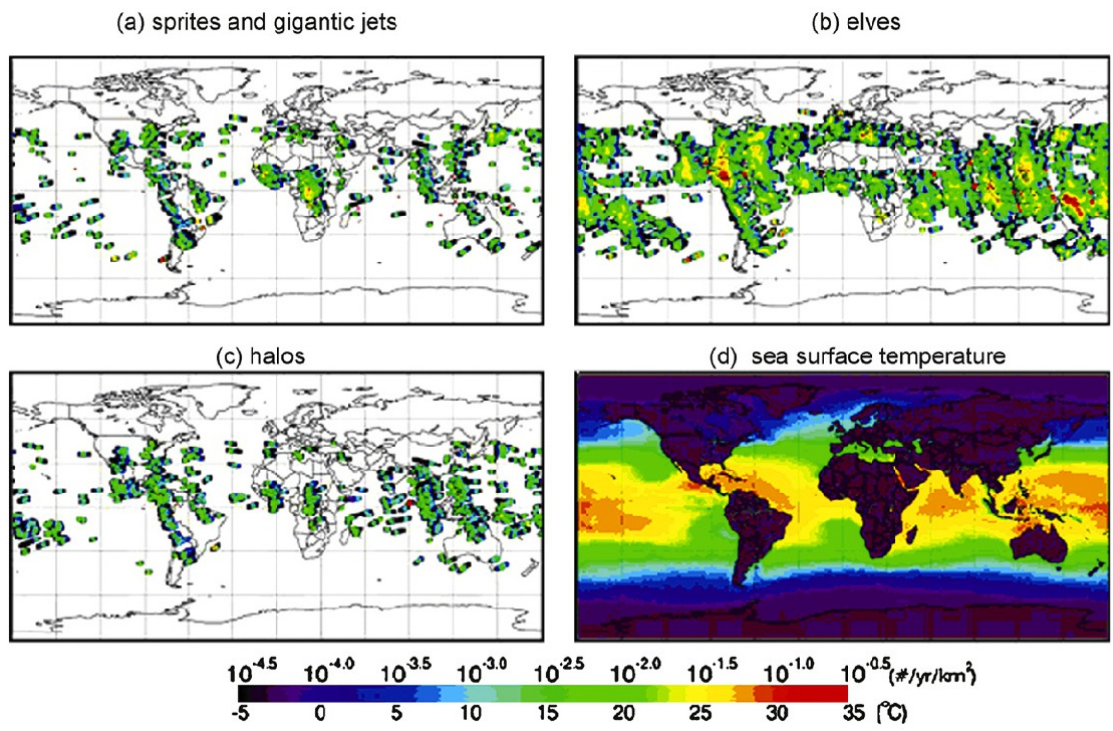


Figure 3: Geographic distribution of TLEs: sprites and GBJs jets (a); elves (b); halos (c) and the sea surface temperature (d), from Ref. [16].

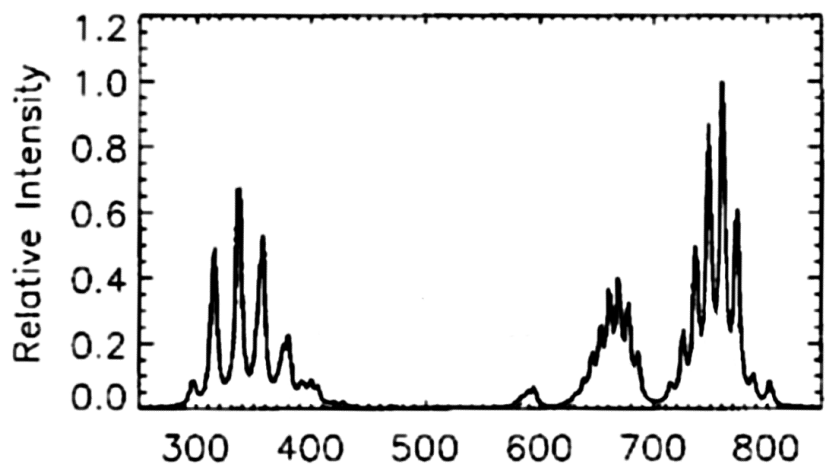


Figure 4: Sprite spectrum at source. Wavelength in nanometers is represented on the X axis. The $2P N_2$ band is of particular interest for FOG measurements. Other TLEs have similar spectra (adapted from Ref. [15]).

typically distributed over tens of milliseconds. The expected number of photons during the burst in the overlooking pixel is therefore about 3×10^8 , probably saturating the detector. However, since the GBJs must be pointing towards FOG, the event rate is very low, below ~ 1 event per month of FOG operation, concentrated on the central pixels given the directionality of the GBJ emission.

While Sprites are less energetic events than GBJs, their upward emission is more isotropic, making them a more favorable case for FOG. The total flux at source is estimated to be about

$$\mathcal{F}_{\text{sp}} = 10^{12} \frac{\text{ph}}{\text{cm}^2 \text{ s sr}}$$

produced at typical altitudes of ~ 30 km[18], integrated over the full emission spectrum. Given Fig. 4, about 35% of the photons should be in the NUV band. Assuming a typical sprite duration of 17 ms, the expected number of photons in a FOG pixel pixel should be

$$N_{\text{sp}} \simeq 7 \times 10^4 \text{ ph},$$

with an occurrence rate of ~ 8 events per day of FOG operation.

1.2.2 Tatiana UV Flashes

The Tatiana satellite[8] discovered various terrestrial flashes in UV light[19]. Given the similarity of FOG with Tatiana, a special look at these flashes is given here. Some typical flashes can be seen on figure 5, together with their distribution on Earth.

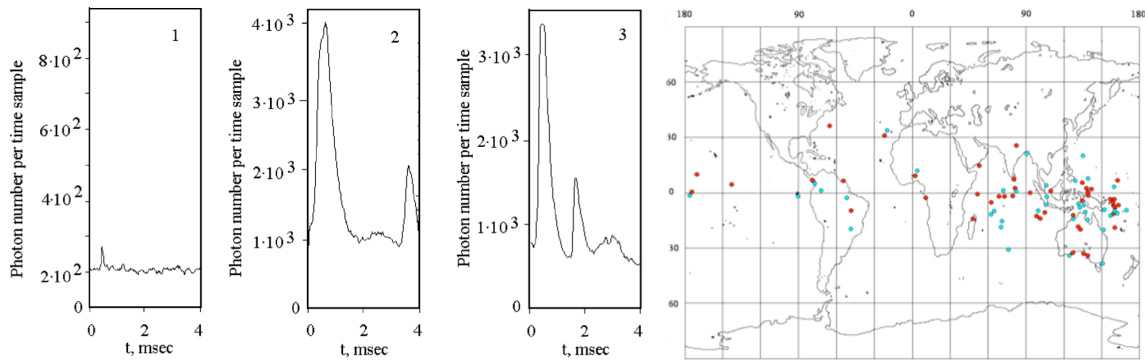


Figure 5: Terrestrial UV flashes observed by Tatiana. Left: some typical flashes time behaviour. Right: flashes distribution on Earth (red: short bursts, 1-4 ms, blue: long bursts, 10-64 ms).

There is no agreement in the community whether these flashes can be explained by the TLE introduced in 1.2.1. Alternative explanations involve changes in the geomagnetic field due to tectonic movements which would provoke precipitation of the cosmic rays trapped in the Van Allen belts in the atmosphere. This would allow to detect precursors to earthquakes. While TLEs seem a more likely explanation, the observation of more flashes from a fixed position in the sky will provide valuable data to advance in this field.

In [8], the number of photons detected by Tatiana in these flashes is reported to be about 10^4 to 10^5 . Assuming the size of the burst is such that it is fully in the field of view of Tatiana (most likely and most pessimistic case), the number of photons in one pixel of FOG has to be this number corrected for the distance and the collection area of both detectors. With a squared distance ratio of 1420 in favour of Tatiana, a size ratio of 360 in favour of FOG, and another factor of 2 in QE as FOG uses ultra bi-alkali MAPMT, one gets in FOG about half the number of photons seen by Tatiana. Given the short time scale of these bursts (a few ms), they will be clearly visible in FOG.

1.3 Gamma Ray Bursts

Since their discovery at the end of the 60's[20], the Gamma Ray Bursts (GRB) have been of high interest to astrophysicists. A GRB is characterised by a sudden emission of gamma rays during a very short period of time (between 0.1 and 100 seconds). The luminosity reached during this flare is typically between 10^{51} and 10^{55} ergs, should the emission be isotropic. The astrophysical source of these bursts is

still not clear but candidates would be coalescence of compact objects (neutron stars), and mechanisms based on internal shocks of relativistic winds in hypernovae. Many reviews are available, and one can refer at [21] and subsequent references for more information.

Many satellites and ground observatories are active in the field of GRB detection and characterisation. Here we will address the possibility of detecting a GRB by a sudden flash of fluorescence of the whole atmosphere, as the GRB photons reach the Earth and cascade in the upper layers of the atmosphere. This study is based on [22] where detecting a GRB in fluorescence from the ground level was considered.

Using the equations of [22], and considering only the low energy fluorescence, as this is the one produced in the upper atmosphere (see [22] for a detailed study of the two components of the fluorescence expected from a GRB), one gets that the typical flux of fluorescent photons is $200 \text{ cm}^{-2} \text{ sr}^{-1} \text{ s}^{-1}$, for a reference burst of $1 \text{ MeV} (E/\text{MeV})^{-2}$.

In order to estimate the signal expected for a wide range of GRBs, the SWIFT catalogue of GRB was used[23]. The relevant parameters are the burst duration T_{90} and the BAT Fluence in the 15-150 keV range. The reference burst considered above has a fluence of $10^{-4} \text{ erg cm}^{-2}$ in this energy range. A $10^{-7} \text{ erg cm}^{-2}$ burst (the reference of the SWIFT catalogue) would therefore produce a fluence of fluorescence photons of $0.2 \text{ cm}^{-2} \text{ sr}^{-1}$. Given the diameter of the FOG mirror of 15 cm, this would translate into a fluence of about one photon for the whole field of view.

Even the most powerful bursts seen by SWIFT would only produce up to a thousand photons in FOG over periods of time of tens of seconds. There is therefore low expectation to see any GRB with this method unless a short and bright burst is observed.

2 Detector Description

Given the distance from the GEO orbit to the Earth, a collecting surface will be needed. The basic design is a telescope with a mirror of about 15 cm of diameter illuminating a MAPMT. Each channel of the MAPMT will be read independently at a high frequency rate. The design in itself has to be compact and of low weight.

2.1 Optics design

The requirements for the optical system is a moderate field of view of up to 14.4° , with the maximum aperture possible given the low light levels. Given the big size of the individual pixels of the camera, there is no need for a complex design and a single mirror system with a diaphragm can be used.

The optical system selected is an on-axis lens-less Schmidt design, with a 19 cm diameter spherical mirror of 21.4 cm of curvature radius, with a 14 cm diaphragm located at the centre of curvature of the mirror, while the MAPMT will be located close to the focal point, at 10.3 cm from the mirror, where the spherical aberration is minimised. The PSF has been checked for all angles of incidence and is concentrated in a spot 2 mm in diameter, with a 3.1 mm diameter halo. The design is summarised in figure 6.

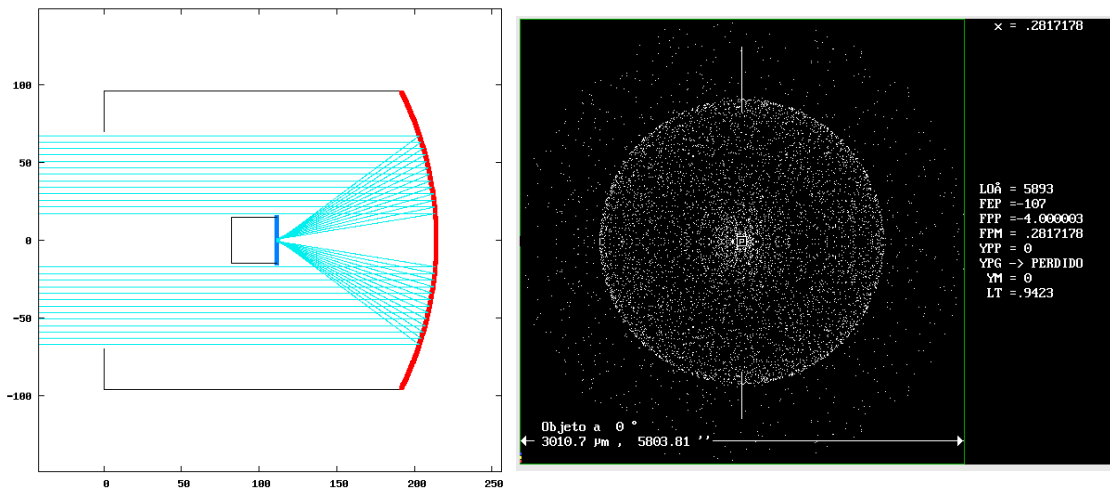


Figure 6: Left: design proposed for FOG (see text for details) with paraxial ray tracing. MAPMT is at centre, and the entry of the tube is cut by the diaphragm. Dimensions are in millimetres. Right: PSF corresponding to this situation, as determined by an optic program from Enrique Campitelli.

The fluorescence emission lines of N_2 can be seen on figure 7. Below about 310 nm, the Earth atmosphere is opaque to photons due to the Ozone absorption. One therefore needs a UV filter to cut light with wavelength above 400 nm. Many commercial or home-made filters have very fast transition and could be used.

2.2 Electronics

2.2.1 Analog electronics

A 16 pixels MAPMT will be used as a camera. The selected one, R8900-200-M16MOD-UBA is a ultra bi-alkali photo-cathode with an enhanced quantum efficiency of 43% at peak, and rugged dynodes to make it appropriate for space launching. This phototube from Hamamatsu Photonics K.K. has been tested for its quantum efficiency, single photo electron (SPE) response, and vibration resistance up to $17 G_{rms}$ [25], making it an adequate solution for a space-borne UV telescope.

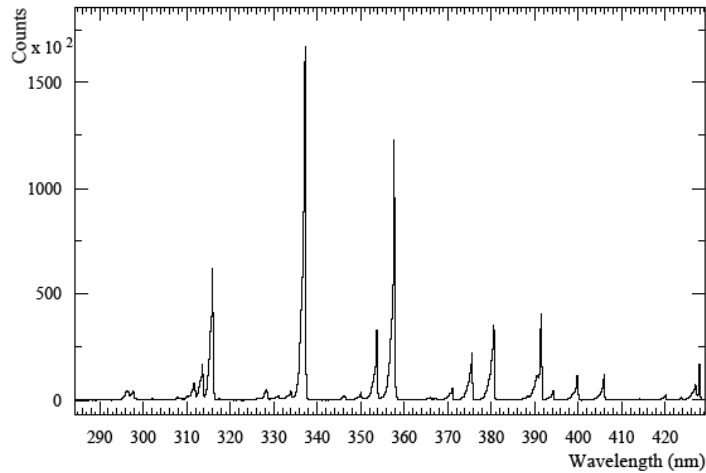


Figure 7: Fluorescence spectrum in the UV as measured by the AIRFLY experiment[24].

Given the photon fluxes to detect (from KHz to MHz, see 1), measurements have to be made at the SPE level. For each of the 16 outputs of the MAPMT a discriminator will be set in order to feed the digital electronics (FPGA) with a low or high level, depending whether a photon was detected or not. The 16 discriminators will be controlled by a single DAC. Given the non uniformity of the gain and SPE response, this means the efficiency of the detector will not be uniform over the 16 pixels and this will have to be measured by the calibration (see 3.2.1) in order to compensate for this non-uniformity offline. It would make the design much more complex to have 16 individual thresholds, hence the choice to go for only one DAC and offline corrections. This design is very similar to one operated in the AMIGA project of the Pierre Auger Observatory where a 8x8 MAPMT is used in counter mode to detect SPE[26]. The electronics in AMIGA is modular and uses daughter boards each in charge of 8 channels as can be seen on figure 8 due to the high number (64) of channels. SPE detected by the MAPMT are converted into squared pulses of less than 2 ns of rise and fall time to be read directly by the FPGA as digital 1 or 0.

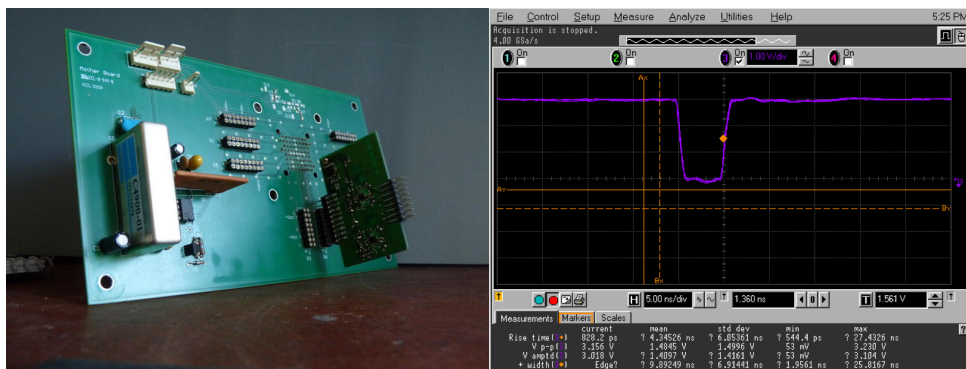


Figure 8: Left: AMIGA project board. It is operating in a similar way to what FOG will be, but with 64 channels of an 8x8 MAPMT. Right: analog response to a SPE pulse.

Based on this AMIGA design, a prototype single board for 16 channels has been designed and the drawings can be seen on figure 9. It is a 4 layer board that has to be fed with ± 3 V and ± 12 V. The power consumption for the analog part described here has been calculated to be around 980 mW. The MAPMT will be connected to the analog board via a ribbon cable. Since the 64 channel board of AMIGA has been in operation for more than 6 months in the Pierre Auger Observatory, this 16 channel board is not expected to present major issues.

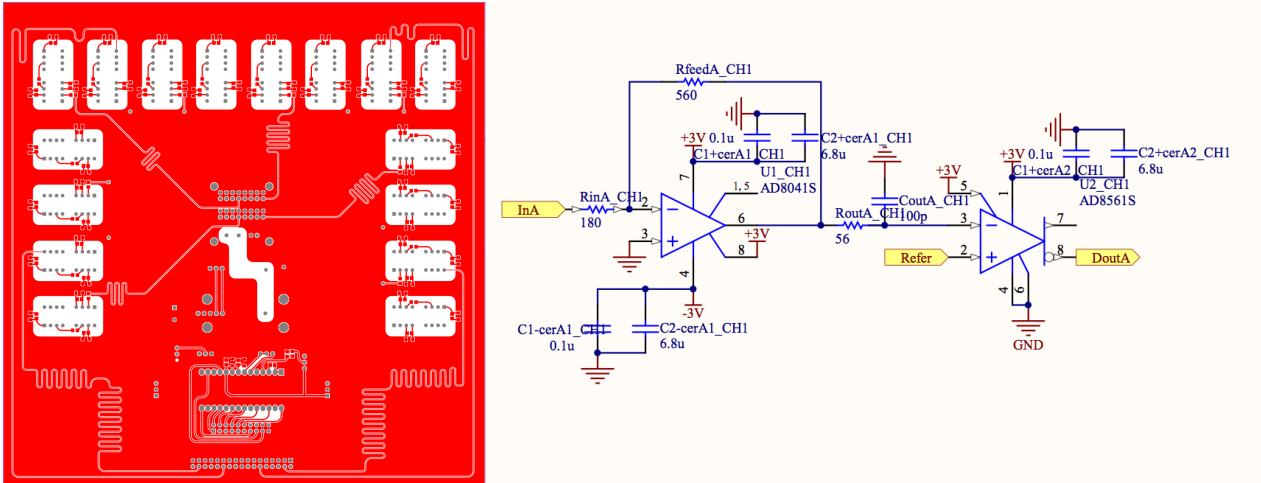


Figure 9: Left: Top layer of PCB for prototype board. Right: Schematics of one channel.

2.2.2 Digital electronics

The discriminated lines are sent to an FPGA for the digital processing. An Actel FPGA will be used. As the detector in itself is quite versatile and has various different scientific goals, a reprogrammable FPGA such as the RT ProASIC3 RT3PE600L would be an ideal solution. In any case, a RTAX or RTSX-SU can also be considered. Given the width of the SPE one wants to detect, a high frequency above 200 MHz is needed.

The FPGA will have 16 input dedicated to the 16 pixels of the MAPMT. In order to avoid using ADC and lower the power requirements, the input will be directly the discriminated lines. These 16 inputs will be 1 if no signal was found above the discrimination threshold, and 0 if a signal was found. As the SPE signals from the MAPMT are short, one expects to get a 0 for about one time bin when a photon is detected. This will be checked by the online calibration (see 3.2.1).

The FPGA will be in charge of the data acquisition, operating in parallel in various DAQ mode in order to fulfil the different scientific objectives. More details on what is expected from the FPGA data processing can be found in 3.2. It will regularly push the data through the RS422 lines to a central processing unit. The CPU will be in charge of selecting from the various data flows which are more relevant and should be sent to Earth. The FPGA will be controlled by the CPU in order to enter in calibration mode or normal DAQ, and to set up the MAPMT high voltage (HV) and the discrimination DAC.

The digital board will also be in charge of converting the entry voltage provided by the satellite to the voltages needed by the FPGA and the analog board, using DC-DC converters.

During the prototyping phase, a ARM Cortex-M1-enabled ProASIC3L development kit will be used as the digital part of the detector.

2.2.3 Power consumption and temperature considerations

Given the fact that FOG will only take data when shadowed from the Sun by ARSAT-1 (see 3.1), the power consumption is greatly reduced. Furthermore, power will be needed when the ACTA box is at night, making it easier to dispose of heat.

DAQ will start well after the ACTA box has been shadowed by the Sun (this happens at noon local time) as one needs the atmosphere below FOG not to be illuminated. This would be typically at 20h30 local time (which means 8h30 after the ACTA box swept into shadow) and finish at about midnight, when ACTA starts to be illuminated again by the Sun. This means the operation will be done during what is likely to be the coldest period and some heaters may be needed for the MAPMT and electronics

to operate properly. We plan to use Polyimide (Kapton[®]) Thermofoil[™] heaters[27] if necessary.

The temperature of the FOG detector will be measured in 2 points, the first one located at the MAPMT level and the second one in the analog electronic board. In case the digital board is separated from the analog one, a third temperature sensor will be used.

The average power consumption over a day of FOG will therefore be 15% of the DAQ power consumption, plus the temperature regulation power. It should be at most 2 W when no DAQ is running and ACTA is in shadow if heating is necessary, and increase to less than 7 W (including thermalisation) in DAQ mode, for a total below 50 W h daily (equivalent to an average power consumption below 2 W).

2.3 Packaging

The design chosen is a 190 mm diameter tube, 230 mm long, hosting the optical system and the MAPMT (see figure 10). The analog electronics will be installed in a 20 mm tall box located below the tube. The digital FPGA can either be located along with the analog board or in a separate board that could be plugged in ACTA.

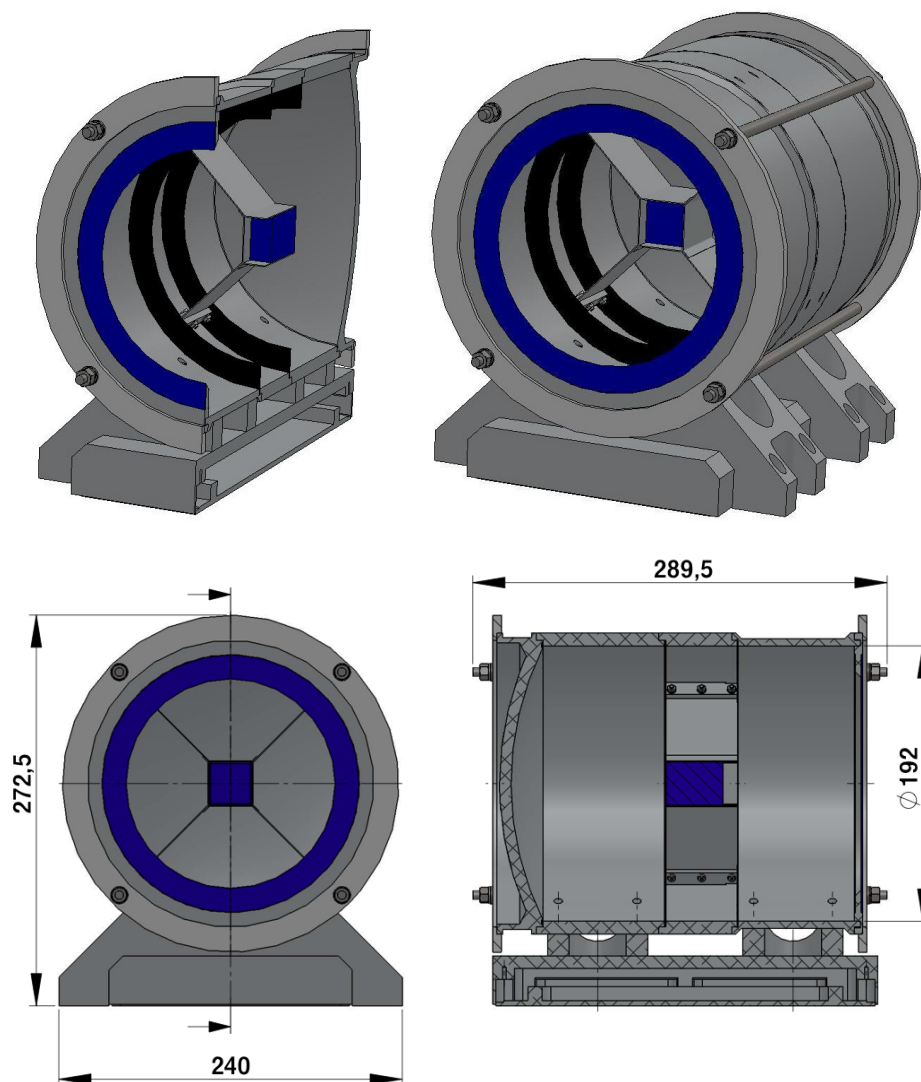


Figure 10: The FOG detector. Dimensions are in millimetres. The MAPMT is fixed in the central position in the tube by a 4 arms structure. A diaphragm is placed at the entry of the tube, and 2 wafers are inside the tube to limit parasitic light. The electronics box is placed below the tube.

The whole package would be located with the electronics board along the satellite, in order to benefit from its shielding. Extra shielding is needed for the exposed PMT not to receive a too high electron radiation from the diaphragmed opening. Its site will be shielded on its back and its sides by High Z material such as tantalum or tungsten. The front is shielded by the mirror and half of the tube, which is 9 mm in order to reduce the electron flux to less than 100 Hz per pixel. Once the location of FOG is determined within ACTA, the main tube will probably have its thickness reduced where significant shielding is already offered.

A model is being worked on in SolidWorks. The current total weight of the design is 8.1 kg, and is expected to be reduced once the location within ACTA is defined.

2.4 Detector Simulation

Through simulation it is possible to perform a complete study of the response of the detector while subject to the space environment of the GEO orbit. Three topics are to be considered during the detector design: (i) the shielding power of different materials to protect the device from radiation damage, (ii) the optical system aberrations for different camera and/or diaphragm size and position, and (iii) the electronic response. The presented analysis were carried out by means of the Geant4 package[28], a well established and proven software for detector simulation. The concept of the simulation is schematically shown in figure 11: depending on the shielding material selected, particles trapped in the outer radiation belt can traverse the detector enclosure increasing the noise and disturbing the UV signal; these penetrating particles can also cause serious damages to electronic devices.

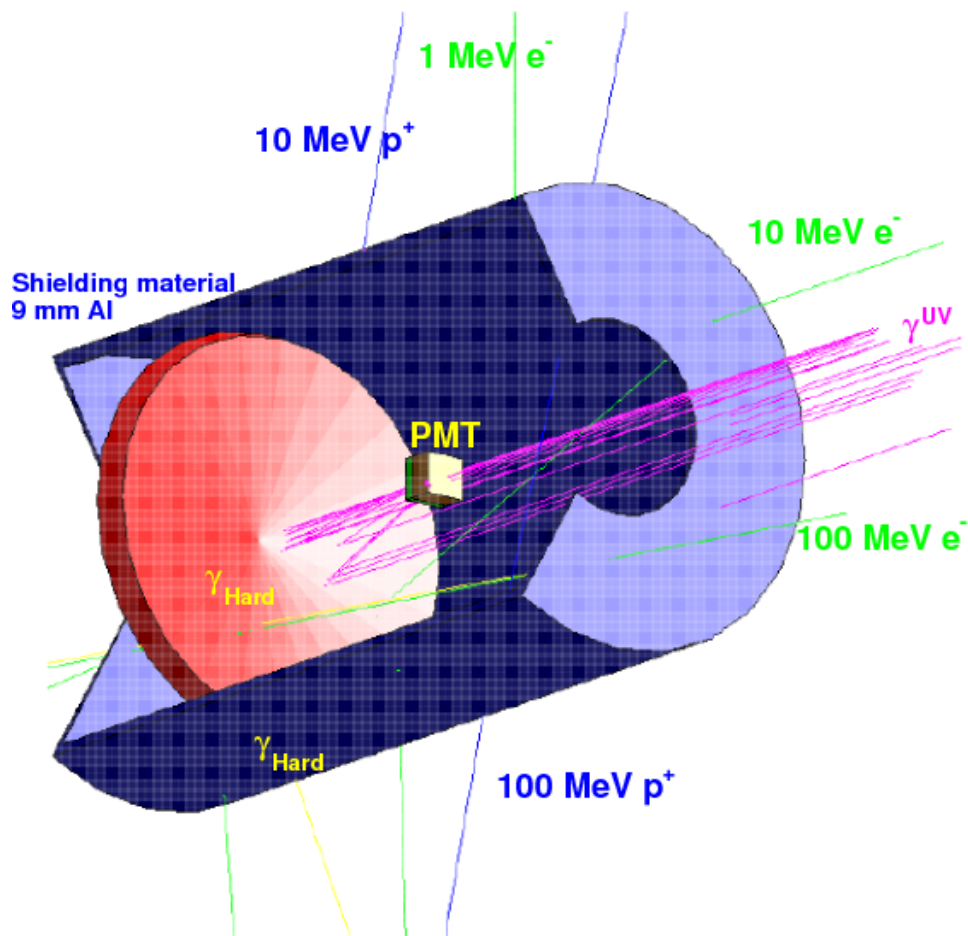


Figure 11: Detector simulation scheme.

1. Shielding materials

Energetic particles can lead to detector failures through radiation damage. Among others, one of special concern, is the radiation environment at geostationary orbit. In this space region most radiation is due to high energy trapped electrons of the outer Van Allen belt which extend from $2 R_E$ to $8 R_E$. Other free ions are also present in this region even though with much lower density.

As an example, we show in figure 12 the shielding power of an aluminium (*Al*) layer of three different thicknesses (0.1 mm, 1.0 mm, and 5.0 mm) for vertically impinging electrons with energy 10 keV, 1 MeV, and 100 MeV. The relative electron energy distributions after traversing the material sheet are also shown.

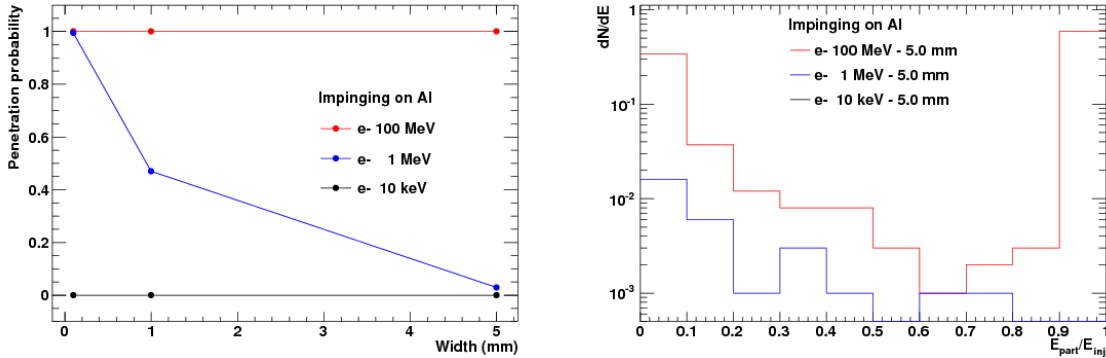


Figure 12: Left: Penetration probability as a function of shielding material thickness for the *Al* case. Right: Relative energy distribution of electrons after traversing a shielding layer of 5 mm of aluminium.

2. Optical system

Using the expected UV flash rates and the spectra of particles trapped at the geostationary orbit it is possible to simulate the expected signal-to-noise ratio for different optical system parameters. The aberrations due to the optical reflection system can also be properly studied to optimise the design, and it is important to check the spot size in the camera plane.

If UV flashes coming from Earth arrive forming an angle θ with respect to the optical axis, the spot will move around the camera pixels and the aberrations will be enhanced. All these effects have been checked with the design shown in figure 11, with results in good agreement with the optical program used for the optic design.

3. Electronic response

The electronic simulation has not been implemented yet but will be developed based on the experience acquired in the simulation of the Pierre Auger Observatory electronics.

3 Detector Operation

3.1 Duty Cycle

FOG will take data as long as no pixel of its MAPMT is exposed to an amount of light larger than what the atmosphere would emit on a full moon night.

As FOG will observe a large portion of the Earth, it is important to compute the data taking period. Even if the sun does not illuminate the area observed by FOG, light diffused through the atmosphere could produce enough light to make measurements useless, or, worse, harm the detector.

A simple calculation of the duty cycle can be done considering that on a given spot on Earth, the amount of light received by diffusion in the atmosphere roughly depends only on the angle of the sun with respect of the vertical, that we will call α . Clearly, at sunrise or sunset this angle is around 90° , but this is not enough to guarantee the absence of diffuse light. The astronomical twilight, defined when this angle is between 102° and 108° , defines the transition period to ideal measurement. Actually, data can also be taken in what is called the nautical twilight, where the angle is between 96° and 102° . When the sun is at about 98.5° , the amount of light diffused in the atmosphere is roughly equivalent to a night sky lit by full moon.

The face of Earth exposed to the satellite is 180° . When the Sun is exactly on the opposite side of the Earth, the portion of Earth that is lit by the diffused light is a ring of $\alpha - 90^\circ$ of angular width. This means the angular width β in shadow where a proper measurement can be obtained is $\beta = 180^\circ - 2 \times (\alpha - 90^\circ)$. The field of view of the detector has to be smaller than β . For $\alpha = 108^\circ$, one gets an area on Earth in shadow of 144° . As the rotation of the Earth is 15° per hour, the duty cycle t will be given by the difference between the shadow angular width and the detector field of view γ , divided by this 15° per hour:

$$t = \frac{180^\circ - 2 \times (\alpha - 90^\circ) - \gamma}{15^\circ} \text{ hours}$$

With $\gamma = 60^\circ$, a reasonable field of view on Earth, one gets:

- Dark night: $t = 5\text{h}36$
- Dark night and Astronomical twilight: $t = 6\text{h}24$
- Up to Nautical twilight: $t = 7\text{h}12$
- Up to equivalent of full moon: $t = 6\text{h}44$

Using a γ of 90° one decreases these values by 2 hours.

These values are valid for equinoxes and the equatorial pixels. They will be decreasing when moving towards the poles or away from these dates. The effect is however small as long as the field of view of the detector is small enough so that the polar diffused light does not reach the area of observation. This would happen at solstice time for the top pixels for $\gamma = 180^\circ - 2 \times (\alpha - 90^\circ) - 2 \times 23.4^\circ$. Taking $\alpha = 108^\circ$ for dark night, one gets a maximum γ of about 97° . By keeping the field of view γ below 97° , one only gets secondary order corrections greatly reduced by the fact the corner pixels of the MAPMT are blinded.

One important source of parasitic light will be the Sun. While the Sun will never be in the field of view of FOG, any reflection of it in the FOV would be catastrophic. One could try to reduce this parasitic light with wafers in the optical system before the diaphragm, but this would greatly increase the size of the apparatus and any scratch on the tube could turn into a reflection spot rendering the whole FOG useless. However, the location of FOG on the East face of the ARSAT-1 satellite gives FOG 12 hours of night when ARSAT-1 itself acts as a shadow from the Sun. We will therefore limit our duty cycle by 50% by taking data only when the Sun is shadowed by the satellite.

In these conditions, if a 60° field of view is selected for the instrument and data is only taken when ARSAT-1 shadows the detector, the duty cycle of FOG will be of about 3h30 daily, of which 2h45 are dark night equivalent.

3.2 Online data processing

Even without telemetry limits, it is clear that the data has to be processed online as one cannot keep counting rates of each pixel every microsecond. Depending on the science to be done, the processing will be different. We will therefore consider the different scientific cases studied previously and describe the online data processing associated to each.

3.2.1 Calibration

The first data processing will be a calibration run. This will be done at the beginning and at the end of a night of observation. The first task is to find the threshold for the discriminator in order to maximise signal to noise ratio on the SPE. This will be done in two steps. First a mid range threshold will be set for the discriminator and the High Voltage will be varied measuring event rate to find the SPE detection plateau. Then, once the HV is set, a fine tuning of the threshold will be done by taking data at varying thresholds and looking again for the SPE detection plateau.

It is important to note here that both the HV and DAC threshold are common to all 16 MAPMT channels. The 16 channels will therefore exhibit different behaviour and the calibration will allow for offline correction of the counts obtained to calibrated uniform counting values. The HV and DAC threshold will be selected so that all pixels are above the SPE plateau.

In addition to the start and end of night observation, when the FPGA is set in calibration mode, these data will be taken every 10 minutes and every 5 degrees of temperature change, in order to quantify the MAPMT and electronics response throughout the night of observation.

Once HV and thresholds are set and their behaviour with temperature understood, one has to determine the average number of bins that are above threshold for a SPE. This will be done by making simple histograms for each pixel of how many consecutive pixels are over threshold. The average value of this histogram will tell us how many time bins occupies an average SPE, and this will be used to convert total FPGA counts into SPE.

3.2.2 Fluorescence background

A first processing will be done pixel by pixel. For each pixel, an histogram of the amount of photons detected every millisecond will be done. These histograms will be kept every minute, and added into hourly histograms. They will be used for generic statistical studies.

Then, pixel correlations will also be studied. An histogram of the number of pixels hit at the same moment (same moment being within one time bin difference) will be built. For the histograms of 2 pixels hit at the same time, difference will be done between 2 adjacent pixels and 2 distant ones. All these histograms will also be built discriminating normal pixels and blinded ones. This will be used in search of coincidences above casual ones as well as for crosstalk measurements for calibration issues.

Time correlation will also be studied. Since flashes will be treated by other data flow, the analysis here will be limited at looking at the time difference between 2 photons detected by the same pixel, in search for any specific pattern.

3.2.3 Terrestrial flashes

As Terrestrial UV flashes are rather short, the amount of counts every tenth of millisecond will be registered in a circular buffer of 128 entries for each pixel. A flash will be defined by a time over threshold trigger. The rate of event on one pixel will have to be above a specific number of counts with respect of the background rate in a specific number of bins in the determined window of time. In this case a buffer of 0.1 second of data will be kept after the trigger has been latched, and then analysed in order to reduce it to a relevant time trace. The algorithm will reduce the time in order to obtain the highest signal to noise ratio (with noise being the square root of the baseline rate, while signal is the sum above this baseline).

All these traces will be kept by the CPU in a circular buffer and be sent to Earth when telemetry is available.

3.2.4 Gamma Ray Bursts

As it is unlikely that FOG detects any GRB, this data analysis will be kept in low priority mode. Here, one looks at flashes on all pixels, and on longer time scales than above. The amount of counts every millisecond will be recorded for 1024 time bins per pixel, and the amount of count per second will also be kept for a duration of 512 seconds in order to optimise triggers both for short or long GRB. Two different time over threshold will be applied and asked to trigger on at least 4 pixels in the same time window (but not necessarily in coincidence, as the photons detected are from different primaries and the time coincidence is expected at the level of the second). If a trigger is found, the 16 traces will be kept for the relevant time window and sent to the CPU to be sent to Earth when telemetry is available.

3.3 Fault tolerance

Fault tolerance is a very important part of the DAQ. As the data of FOG is not mission critical, most of the implementation of fault tolerance will be based on safety considerations with total shutdown and restart upon fault detection. A cold start will therefore check all the relevant software and hardware parts before startup.

The main critical apparatus is the MAPMT, and one must ensure no HV will be set when the light background is high. Even if there will never be direct exposition of the PMT to high level of light, turning on the HV when the atmosphere is lit by the Sun or when the ACTA box is lit might damage permanently the MAPMT. In particular one should try to avoid a SEU in the DAC control of the HV, as this could have dramatic consequences. The low voltage to the HV module will be controlled by a multiple redundant bitmask, including bits set by the remote CPU and not the FPGA, to ensure no such issue happens.

The digital part will have a hardware watchdog which will cold reset the board in case the FPGA does not reset it every second. It will be built with triple redundancy to ensure no SEU can affect it.

The software running in the CPU and in communication with the FPGA based DAQ will also operate a software watchdog, and interchange data with the FPGA every second to ensure the communication link is operating properly. In case there is no response, a hard reset will again be issued.

Finally, the FPGA will operate with triple redundancy and majority vote system. In case a reprogrammable FPGA is used, the FPGA will be reprogrammed when the number of errors detected by the vote system passes a specific threshold.

3.4 Telemetry

Upon starting, a large portion of the Telemetry will be used for calibration. This portion will be reduced at only calibration checking runs later on.

Calibration data are SPE plateau histograms (100 entries, 1 byte each) both in HV and threshold, as well as average SPE width for each channel (5 entries, 1 byte each). This would represent 1.7 kB of data, plus some generic header. One expects therefore less than 2 kB per calibration run.

Fluorescence histograms will be reduced to 30 bins of 1 byte count each (including an overshoot bin). Hourly histograms for each pixels will be transferred, for a total of about 500 bytes per hour. Then every minute the minute histogram of one pixel will be transferred in different modes (either always the same pixel, or the sequence of all pixels one at a time), for an extra data flow of 30 bytes per minute.

Pixel correlation, time difference histograms and monitoring information (temperatures, voltages) will be send on an hourly bases, with 2 kB allocated for these data.

Terrestrial flashes will be typically a succession of 100 2 bytes counter, and are expected to happen only scarcely, therefore not contributing for much in the total data flow. Assuming a maximum of 100

bursts detected in a night of observation (to be compared with the ~ 8 expected from known TLE, see [1.2.1](#)), one gets 20 kB of data per night.

GRBs would typically last for 1000 time bins for 16 pixels, with 2 bytes counters, for a total of 32 kB. As one does not expect to detect more than a few GRB in the detector lifetime, it can be totally neglected for the total data flow determination.

Considering a full night of observation, one therefore expects a total amount of data below 40 kB. The total telemetry in normal DAQ mode should therefore be ~ 4 bps.

4 Organisation, Costs and Schedule

4.1 Project Organisation

The FOG detector work is supervised by its principal investigators. They are in charge of the whole project and its interface with the ACTA team. They are also in charge of the organisation and task distribution within the project. Given the short timescale of the project, there is no change foreseen in the organisation. Should such changes be necessary, the PIs would determine it. The PIs of the project are:

Principal Investigators: Xavier Bertou, Mariano Gomez Berisso

The work on FOG is divided in various areas, each of them having a coordinator. The coordinator is responsible for the development of his task within the resources available and to meet the deadlines planned in this document. He is to report to the PIs on a monthly base. The following areas have been defined:

1. Physics studies
2. Optics and mechanics
3. Analog electronics
4. Digital electronics and communication
5. Monte-Carlo simulation
6. DAQ, calibration and operation

Each task is described below with the relevant work expected from it.

Physics studies

Coordinator: Hernán Asorey

This task is in charge of estimating the signals expected from the various physics phenomena that can produce UV fluorescence photons in the atmosphere. It has also to provide an estimation of the background flux of particles that could produce parasitic signals.

Optics and mechanics

Coordinator: Mariano Gomez Berisso

This task has to design the optical and mechanical system of the FOG detector, and build the prototype. It is also in charge of all the tests to be done from the optical, mechanical and thermal dissipation point of view.

Analog electronics

Coordinator: Manuel Platino

This task has to design and produce the analog electronics for the FOG detector, characterise it and guarantee its performances in presence of the environment of ARSAT-1, taking into account the particle radiation background and the electromagnetic radiations produced by the various elements of the satellite.

Digital electronics and communication

Coordinator: Miguel Sofo Haro

This task is in charge of the design and production of the digital electronics board, as well as its programming. The interface with the on-board computer of ACTA and the data flows are also responsibility of this task.

Monte-Carlo simulation

Coordinator: Federico Sanchez

This task has to run a complete simulation chain of the detector using a well proven program (such as Geant4). This includes both the reaction of the detector to UV photons as well as the background noise produced by cosmic rays in the detector.

DAQ, calibration and operation

Coordinator: Xavier Bertou

This task is in charge of defining the algorithms to be operated in calibration, idle and run modes. Cold start and fault tolerance will be addressed to ensure a proper operation in the high radiation environment.

4.2 Project Schedule

The FOG detector design is already well underway. There are no known barriers to the successful construction and operation of a prototype. All the expertise needed is present and similar projects have been developed in the past.

In order to construct an engineering model, collaboration is foreseen with INVAP and the Universidad de La Plata engineer group, which have a rich experience in the building of satellite equipment.

The following milestones are foreseen:

- April 2010: prototype analog board in operation
- April 2010: dummy mechanical structure built
- June 2010: integration MAPMT - analog board - FPGA prototype board
- June 2010: prototype digital board in operation
- July 2010: full prototype in operation
- August - September 2010: engineering model construction
- October 2010: engineering model testing starts

Given the tight schedule, all the parts foreseen for the engineering model will be bought before end of April 2010. Any component change imposed by the June-July testing period would imply a critical delay to the engineering model. Any change of this schedule due to unforeseen difficulties will be communicated by the PIs to the ACTA team upon notice.

4.3 FOG Costs

It is expected that all the costs will be covered by the PID 2008-00008 “*Investigación Básica y aplicada en un Satélite de Órbita GEO (ARSAT): monitoreo de partículas cargadas, fluorescencia terrestre y comportamiento de paneles solares de fabricación nacional*”. In case some items could not be covered by this project, the task coordinator is responsible for finding the necessary extra funding.

The expected costs for the prototype detector is about US\$15 000, with a third of it for the packaging and a similar fraction for the MAPMT. The completion of an engineering model, not including the engineering model testing, are expected to be at the level of US\$35 000. An approximate breakdown of the costs can be found in table 1.

Prototype detector costs	
Analog board components	\$ 600
Analog board manufacture and testing	\$ 150
Digital FPGA test board	\$ 1000
Mechanical structure materials	\$ 800
Mechanical structure manufacture	\$ 2500
Optical module	\$ 700
MAPMT	\$ 6500
Integration tests	\$ 1500
Travel and related expenses	\$ 1500
Total	\$ 15250

Engineering model construction costs	
Analog board components	\$ 2000
Analog board manufacture and testing	\$ 1000
Digital board components	\$ 5000
Digital board manufacture and testing	\$ 1000
Mechanical structure materials	\$ 2000
Mechanical structure manufacture	\$ 8000
Optical module	\$ 1000
MAPMT	\$ 8000
Integration tests	\$ 3000
Travel and related expenses	\$ 3000
Total	\$ 34000

Total projected costs	\$ 49250
-----------------------	----------

Table 1: Estimated FOG Costs in US\$, for a total of ~ 50 k US\$.

4.4 Publication policy

A revised version of this document will be published in a peer reviewed journal when the engineering model is operating according to its specification.

Data from FOG will be maintained private for one year to be used by the members of the FOG detector design group and will be then made publicly available. This data release will be done on a yearly bases and a website dedicated to the FOG instrument will offer both the data and an explanatory document. Use of FOG data will have to cite the published FOG design report and acknowledge the FOG design group, Agencia and ARSAT. The exact acknowledgement paragraph will be provided on the data website.

Any publication from a member of the FOG design group using FOG data will be signed by the whole FOG design group with an opt-out policy, and will acknowledge Agencia and the PID 2008-00008, as well as ARSAT.

4.5 Manpower

The following individuals and their respective institutions are committed to the fulfilment of what has been exposed in this design report, and are the current members of the FOG design group:

- **Centro Atómico Bariloche, CNEA/CONICET/UNCuyo/UNRN:** Hernán Asorey, Xavier Bertou, Mariano Gomez Berisso, Edith Losada, Miguel Sofo Haro, Joaquin Venturino
- **Centro Atómico Constituyentes, CNEA/CONICET/UNSAM:** Manuel Platino, Federico Sanchez

The services and technicians depending from these groups will be part of the effort in building both the prototype and the engineering model.

The following individuals are also collaborators in the project, supporting the design and the construction of the FOG detector:

- Enrique Campitelli (former CASLEO)
- Jerónimo Blostein, Pablo Fainstein, Oscar Grizzi, Gerardo Lantschner, Roberto Mayer, Esteban A. Sánchez, Enzo Sauro, Sergio Suarez, Aureliano Tartaglione (CAB)
- Martín Alurralde, Alberto Filevitch (CAC)
- Cesar Bertucci, Sergio Dasso, Marcelo Lopez Fuentes (IAFE)
- All the members of the Unidad de Investigación y Desarrollo GEME of Facultad de Ingeniería, UNLP (coordinated by Pablo Ringegni)

References

- [1] "End to the Cosmic-Ray Spectrum?", K. Greisen, Phys.Rev.Lett 16:748-750,1966
"Upper Limit of the Spectrum of Cosmic Rays", G. Zatsepin, V. Kuz'min, JETPL.4.78,1966
- [2] "Correlation of the highest-energy cosmic rays with the positions of nearby active galactic nuclei", Pierre Auger Collaboration, Astropart.Phys 29:188-204,2008
"Correlation of the highest energy cosmic rays with nearby extragalactic objects", Pierre Auger Collaboration, Science 318:938-943,2007.
- [3] "Observation of the suppression of the flux of cosmic rays above 4×10^{19} eV", Pierre Auger Collaboration, Phys.Rev.Lett 101:061101,2008.
- [4] "USA Astronomy Survey Committee Documents", J. Linsley, 1979.
- [5] "The upgraded TUS space fluorescence detector for study of UHECR", G. Garipov et al., 36th COSPAR Scientific Assembly (2006).
- [6] OWL website: <http://owl.gsfc.nasa.gov/>
- [7] "JEM-EUSO: Extreme Universe Space Observatory on JEM/ISS", Y. Takizawa et al. Nucl. Phys. B Proc. Sup. 166, 72 (2007)
See also www.euso-mission.org
- [8] "UV radiation from the atmosphere: Results of the MSU "Tatiana" satellite measurements", G. Garipov et al., Astrop. Phys. 24, 400 (2005)
See also cosmos.msu.ru
- [9] O. H. Vaughan, et al. "Recent Observations of Lightning Discharges From the Top of a Thundercloud Into the Clear Air Above." Journal of Geophysical Research 94, no. D11 (1989): 13179-13182.
- [10] W. A. Lyons, "The meteorology of transient luminous events, an introduction and an overview." In Sprites, Elves and Intense Lightning Discharges, 398. Corte, France
- [11] M. Sato et al. "JEM-GLIMS Mission." In Workshop on Coupling of Thunderstorms and Lightning Discharges to Near-Earth Space, 1-24. Corte, France, 2008.
- [12] J. M. Thomas et al. "A Very Active Sprite-Producing Storm Observed Over Argentina." Eos, Transactions American Geophysical Union 88, no. 10 (2007): 117.
- [13] E. Blanc, "Space observations of Transient Luminous Events and associated emissions in the upper atmosphere above thunderstorm areas." Comptes Rendus Geosciences (2010): 1-11.
- [14] S.B. Mende, et al. "Spacecraft based studies of transient luminous events." In Sprites, elves and intense lightning discharges, Martin Füllekrug, Eugene A. Mareev, and Michael J. Rycroft, 123-149. Netherlands: Springer, 2006.
- [15] G. Milikh et al. "Spectrum of red sprites." Journal of Atmospheric and Solar-Terrestrial Physics 60, no. 7-9 (1998): 907-915.
- [16] A.B. Chen et al. "Global distributions and occurrence rates of transient luminous events." Journal of Geophysical Research 113, no. A8 (2008).
- [17] G.M. Milikh and M N Shneider. "Model of UV flashes due to gigantic blue jets." Journal of Physics D: Applied Physics 41, no. 23 (2008): 234013.

- [18] R. Roussel-Dupré and AV Gurevich. "On runaway breakdown and upward propagating discharges." Journal of Geophysical Research-Part A-Space Physics-Printed Edition 101, no. 2 (1996): 2297-2312.
- [19] "Ultraviolet flashes in the equatorial region of the Earth", G. Garipov et al., JETP Letters 82, 185 (2005)
- [20] Kleidesabel et. al, 1973, ApJ 182, 85
- [21] P. Meszaros, 2006, Rept.Prog.Phys. 69, 2259-2322
<http://arxiv.org/abs/astro-ph/0605208>
- [22] R. Aloisio et. al, 2008, Astropart.Phys. 29, 373-379
<http://arxiv.org/abs/0802.1650>
- [23] SWIFT GRB catalogue
<http://tinyurl.com/swiftgrb>
- [24] "Measurement of the pressure dependence of air fluorescence emission induced by electrons", the AIRLFY Collaboration, Astropart.Phys.28:41-57,2007
<http://arxiv.org/abs/astro-ph/0703132>
- [25] "Performance of a multi-anode photomultiplier employing an ultra bi-alkali photo-cathode and rugged dynodes", T. Toizumi et. al, NIM A 604 (2009) 168-173
- [26] "AMIGA, Auger Muons and Infill for the Ground Array", Alberto Etchegoyen et al., ICRC 2007 (#1307)
- [27] Minco Polyimide Kapton® Thermofoil™ heaters
<http://www.minco.com/products/heaters.aspx?id=42>
- [28] Geant4 - a simulation toolkit, NIM A 506 (2003) 250-303
<http://geant4.web.cern.ch/geant4/>